

On superconductivity in armchair carbon nanotubes.

A. Sédéki, L. G. Caron, and C. Bourbonnais

Centre de recherche sur les propriétés électroniques de matériaux avancés., Département de Physique, Université de Sherbrooke, Sherbrooke, Québec, Canada J1K 2R1.

(Dated: November 4, 2018)

We use the momentum space renormalization group to study the influence of phonons and the Coulomb interaction on the superconducting response function of armchair single-walled nanotubes. We do not find superconductivity in undoped single nanotubes. When doped, superconducting fluctuations can develop because of the phonons but remain small and are easily destroyed by the Coulomb interaction. The origin of superconductivity in ropes of nanotubes is most likely an intertube effect. Projections to zig-zag nanotubes indicate a more favorable disposition to superconducting fluctuations.

PACS numbers: PACS numbers: 74.20.Mn, 61.46.+W, 05.10.Cc

Since their discovery by Ijima¹ in 1991, carbon nanotubes have attracted a lot of interest due to their unusual geometry and their structural and electronic properties². Band calculations³ (confirmed by experiments^{4,5}) have stressed the one-dimensional (1D) character of single-wall carbon nanotubes (SWCNT).

Recently Kociak *et al.*⁶ reported measurements on ropes of SWCNT making low-resistance contacts to non-superconducting (normal) metallic pads, at low voltage and at temperatures down to 70mK. The preparation technique they have used yields armchair nanotubes⁷. Their results show signs of superconductivity below 0.55K. The authors predict a purely electronic mechanism. The question we address here is whether or not 1D superconducting fluctuations can exist in single SWNT and if phonons can play any role.

To achieve this, we perform perturbative renormalization group (RG) calculations^{8,9} to analyze the low energy behavior of a (n, n) armchair nanotube. The electronic and phonon parts H_0 and the electron-phonon contribution H_{e-ph} of the Hamiltonian were described in a previous publication¹⁰. We added the Coulomb interaction H_{e-e} ¹³. The electron wavefunctions come from a nearest-neighbor tight-binding model using a π_z orbital on each carbon atom of a sheet of graphene which is rolled up in the proper way to generate an armchair nanotube¹¹. In order to build an effective Hamiltonian ($H = H_0 + H_{e-e} + H_{e-ph}$) for low temperatures, we discard all bands that do not intersect the Fermi level. We then linearize the band energies around the Fermi level, $\varepsilon_{\gamma,p}(k') = (-1)^{\gamma+1}pv_Fk'$ where $k' = (k - pk_F)$, $\gamma = 1, 2$ is the band index, v_F is the Fermi velocity, k_F is the Fermi momentum, and $p = \pm$ is the sign of k . This is shown in Fig. 1. The Fermi level lies exactly at the crossing point for a half-filled band. This is the situation we shall first examine. In the g -ology approach to the RG, both the direct electron-electron and the phonon mediated interactions give rise to twelve independent scattering amplitudes $g_{i,e-e}^{(j)}$ and $g_{i,ph}^{(j)}$ ($i = 1, 2, 4$ and $j = 1, \dots, 4$). Here we have adopted the notation of Krotov¹². The index i refers to the momentum branches (p) and j to the velocity branches (sign of the electron velocity = $(-1)^{\gamma+1}p$)

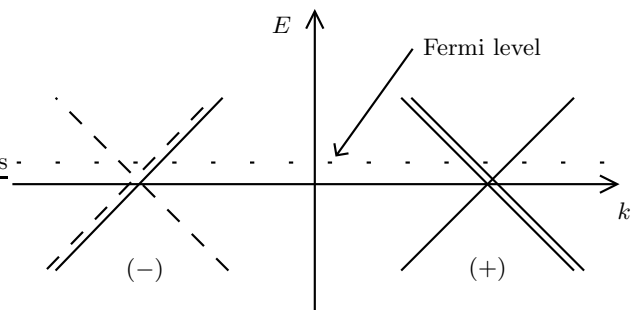


FIG. 1: Energy bands of an armchair nanotube near the Fermi energy. The double and single lines refer to each of the overlapping bands. The Fermi level is at the crossing point in the undoped tube and shifts when doped.

such that 1 = interbranch backscattering, 2 = interbranch forward scattering, 3 = umklapp scattering, and 4 = intrabranch forward scattering. There are no momentum branch Umklapp processes since $4k_F = 8\pi/3a$ in not equal to a reciprocal lattice vector, where a is the tube's unit cell length. The coupling constants $g_{i,e-e}^{(j)}$ were calculated by summing over all tube sites using a Coulomb interaction of the form used by Egger *et al.*¹³:

$$\begin{aligned} g_{1,e-e}^{(1)} &= g_{1,e-e}^{(3)} = b, & g_{1,e-e}^{(2)} &= g_{1,e-e}^{(4)} = b', \\ g_{2,e-e}^{(1)} &= g_{2,e-e}^{(3)} = g_{4,e-e}^{(1)} = g_{4,e-e}^{(3)} = u', & \\ g_{2,e-e}^{(2)} &= g_{2,e-e}^{(4)} = g_{4,e-e}^{(2)} = g_{4,e-e}^{(4)} = u, \end{aligned} \quad (1)$$

where u (u') and b (b') are related to the strength of the bare Coulomb interaction. The ratios $(u/b, b'/b, u'/u)$ vary between $(2, 0.005, 0.01)$ and $(20, 0.01, 0.002)$ when going from a strongly screened to an unscreened interaction. The phonon mediated electron-electron coupling constants in the non-adiabatic regime¹⁴, $g_{i,ph}^{(j)}$, are given by¹⁰:

$$g_{i,ph}^{(j)} \equiv -\frac{2}{\omega_q} g_{e-ph,\gamma}(q) g_{e-ph,\gamma'}(-q) \quad (2)$$

where $g_{e-ph,\gamma}(q)$ is the electron-phonon interaction with

each of the two electrons involved and ω_q is the phonon frequency. One has $q \approx 2k_F$ for backward scattering and $q \approx 0$ for forward scattering. These parameters are valid for temperatures or energies ($k_B = 1$) smaller than the phonon energy.

The symmetry of the electronic functions¹¹ leads to the following sign constraints for the $g_{i,ph}^{(j)}$

$$\begin{aligned} g_{1,ph}^{(1)} &= -g_{1,ph}^{(3)} = g_1 < 0, \quad g_{1,ph}^{(2)} = 0, \quad g_{1,ph}^{(4)} < 0, \\ g_{2,ph}^{(1)} &= -g_{2,ph}^{(3)} = g_{4,ph}^{(1)} = -g_{4,ph}^{(3)} = g_2 < 0, \\ g_{2,ph}^{(2)} &= -g_{2,ph}^{(4)} = -g_{4,ph}^{(2)} = g_{4,ph}^{(4)} = g_4 < 0. \end{aligned} \quad (3)$$

We then perform a one loop RG calculation, which is a generalization of the one band calculation⁸⁹, by considering only the diagrams presenting a logarithmic divergence with temperature, that is with electrons on different velocity branches. The result of this procedure yields the same flow equations for the coupling constants that were found by Krotov *et al.*¹². At half-filling, we use a two cut-off approach¹⁴ with $W > \hbar\omega_{ph}$ where W is the bandwidth and the renormalization starting energy scale while $\hbar\omega_{ph}$ is the phonon energy. For energy (or temperature) scales $E_0 = We^{-\ell} > \hbar\omega_{ph}$, the phonons are adiabatic and the $g_{e-ph,\gamma}$ renormalize only in the random phase approximation. When E_0 reaches $\hbar\omega_{ph}$, the phonons become non-adiabatic, the $g_{i,ph}^{(j)}$ become active and are added to the $g_{i,e-e}^{(j)}$. Contrary to the usual case of a single band crossing the Fermi level, the coupling constants in our case scale towards the strong coupling sector. An analytical solution of the renormalization equations seems to be impossible in the general case, which forces us to resort to a numerical solution.

The important physical properties of the system can be probed through its various response functions. These have the coupling constants as input and measure the relative importance of the underlying fluctuations. It is important to realize that, because of the interband interaction terms ($g_1^{(2)}, g_2^{(1)}, g_i^{(3)}, g_4^{(j)}$), the particle-hole pairs in the Peierls channel and the particle-particle pairs in the Cooper channel will be evolving in both bands. It is thus necessary to define the following response functions in Matsubara-Fourier space

$$\begin{aligned} \chi_\mu^{\kappa,M}(\tilde{q}) &= - \int_0^\beta \int d\tau dx e^{-iqx+i\omega_m\tau} \\ &\quad \times \langle O_\mu^{\kappa,M}(x,\tau)^\dagger O_\mu^{\kappa,M}(0,0) \rangle, \end{aligned} \quad (4)$$

with $\kappa = \pm$, $M = \pm$, and $\tilde{q} = (q, \omega_m)$. The Fourier transforms $O_\mu^{\kappa,M}(\tilde{q})$ are defined by

$$O_\mu^{\kappa,M}(\tilde{q}) = \frac{1}{\sqrt{2}}(O_\mu^\kappa(\tilde{q}) + MO_\mu^\kappa(\tilde{q})^\dagger). \quad (5)$$

In the Peierls channel, one defines

$$\begin{aligned} O_\mu^\kappa(q \approx 2k_F) &= \frac{1}{\sqrt{L}} \sum_{k,\alpha,\beta} [\psi_{1,-,\alpha}^\dagger(k-q)\sigma_\mu^{\alpha\beta}\psi_{1,+,\beta}(k) \\ &\quad + \kappa\psi_{2,-,\alpha}^*(k-q)\sigma_\mu^{\alpha\beta}\psi_{2,+,\beta}(k)]/2, \end{aligned} \quad (6)$$

$$\begin{aligned} O_\mu^\kappa(q \approx 0) &= \frac{1}{\sqrt{L}} \sum_{k,\alpha,\beta} [\psi_{1,-,\alpha}^\dagger(k-q)\sigma_\mu^{\alpha\beta}\psi_{2,-,\beta}(k) \\ &\quad + \kappa\psi_{2,+,\alpha}^\dagger(k)\sigma_\mu^{\alpha\beta}\psi_{1,+,\beta}(k-q)]/2, \end{aligned} \quad (7)$$

in which $\mu = 0$ stands for charge density (CDW) operators and $\mu = 1, 2, 3$, for spin density (SDW) ones. Here σ_0 and $\sigma_{1,2,3}$ are the identity and the x, y, z Pauli matrices, respectively, and $\psi_{\gamma,p,\alpha}(k)$ annihilates an electron of spin α in band γ having momentum k in branch p . We have introduced the parameter M by which we differentiate between on-site and bond-order for charge and spin correlation functions as defined in Ref. 14. In the Cooper channel, one has

$$\begin{aligned} O_\mu^\kappa(q \approx 0) &= \frac{1}{\sqrt{L}} \sum_{k,\alpha,\beta} \alpha [\psi_{1,-,\alpha}(-k+q)\sigma_\mu^{-\alpha,\beta}\psi_{1,+,\beta}(k) \\ &\quad + \kappa\psi_{2,-,\alpha}(-k+q)\sigma_\mu^{-\alpha,\beta}\psi_{2,+,\beta}(k)]/2, \end{aligned} \quad (8)$$

$$\begin{aligned} O_\mu^\kappa(q \approx 2k_F) &= \frac{1}{\sqrt{L}} \sum_{k,\alpha,\beta} \alpha [\psi_{1,-,\alpha}(-k+q)\sigma_\mu^{-\alpha,\beta}\psi_{2,-,\beta}(k) \\ &\quad + \kappa\psi_{1,+,\alpha}(-k+q)\sigma_\mu^{-\alpha,\beta}\psi_{2,+,\beta}(k)]/2, \end{aligned} \quad (9)$$

where $\mu = 0$ are singlet superconducting (SS) operators and $\mu = 1, 2, 3$ are triplet superconducting (ST) ones. It is through these band-entangled operators that our response functions are different from the ones of Krotov *et al.*¹² who only used the untangled ($O_\mu^+ \pm O_\mu^-$) operators. Our definition of the response functions leads to a fundamentally different behavior with temperature.

In order to calculate the evolution of the response functions with the energy scale E_0 (or temperature), we introduce the auxiliary response functions $\bar{\chi}_\mu^{\kappa,M}$ defined through

$$\chi_\mu^{\kappa,M}(\ell, \tilde{q}) = -\frac{1}{\pi v_F} \int_0^\ell \bar{\chi}_\mu^{\kappa,M}(\ell', \tilde{q}) d\ell', \quad (10)$$

where $\ell = \ln(W/E_0)$. We deduce the following renormalization equations

$$\begin{aligned} \frac{d}{d\ell} \ln \bar{\chi}_{CDW}^{\kappa,M} &= \bar{g}_2^{(2)}(\ell) - 2\bar{g}_1^{(1)}(\ell) + \kappa(\bar{g}_2^{(3)}(\ell) - 2\bar{g}_1^{(3)}(\ell)), \\ \frac{d}{d\ell} \ln \bar{\chi}_{SDW}^{\kappa,M} &= \bar{g}_2^{(2)}(\ell) + \kappa\bar{g}_2^{(3)}(\ell), \\ \frac{d}{d\ell} \ln \bar{\chi}_{CDW'}^{\kappa,M} &= \bar{g}_4^{(2)}(\ell) - 2\bar{g}_4^{(1)}(\ell) + \kappa(\bar{g}_1^{(2)}(\ell) - 2\bar{g}_2^{(1)}(\ell) \\ &\quad + M[-\bar{g}_4^{(3)}(\ell) + \kappa(\bar{g}_1^{(3)}(\ell) - 2\bar{g}_2^{(3)}(\ell))], \\ \frac{d}{d\ell} \ln \bar{\chi}_{SDW'}^{\kappa,M} &= \bar{g}_4^{(2)}(\ell) + \kappa\bar{g}_1^{(2)}(\ell) + M[\bar{g}_4^{(3)}(\ell) + \kappa\bar{g}_1^{(3)}(\ell)], \\ \frac{d}{d\ell} \ln \bar{\chi}_{SS}^\kappa &= -\bar{g}_2^{(2)}(\ell) - \bar{g}_1^{(1)}(\ell) + \kappa(\bar{g}_2^{(1)}(\ell) + \bar{g}_1^{(2)}(\ell)), \\ \frac{d}{d\ell} \ln \bar{\chi}_{TS}^\kappa &= -\bar{g}_2^{(2)}(\ell) + \bar{g}_1^{(1)}(\ell) - \kappa(\bar{g}_2^{(1)}(\ell) - \bar{g}_1^{(2)}(\ell)), \\ \frac{d}{d\ell} \ln \bar{\chi}_{SS'}^\kappa &= -\bar{g}_4^{(2)}(\ell) - \bar{g}_4^{(1)}(\ell), \\ \frac{d}{d\ell} \ln \bar{\chi}_{TS'}^\kappa &= -\bar{g}_4^{(2)}(\ell) + \bar{g}_4^{(1)}(\ell), \end{aligned} \quad (11)$$

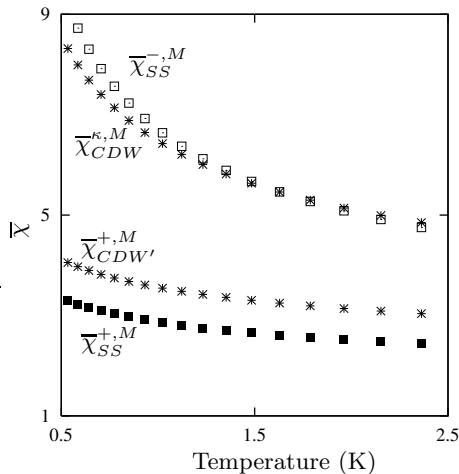


FIG. 2: Typical flow diagram for the response functions of a doped armchair nanotube.

with $\bar{g}_i^{(j)} = g_i^{(j)}/\pi v_F$. CDW' and SDW' refer to the anomalous $q \approx 0$ interband situations while SS' and TS' refer to the $q \approx 2k_F$ ones.

We first report on the calculations without the Coulomb interaction, that is solely with the phonon-mediated effective electron-electron interactions (at temperatures below the Debye temperature for non-adiabatic interactions¹⁴). This was done for arbitrary amplitudes but with the sign constraints given in Eq. (3). We find no sign of a dominant superconducting response in a single-walled armchair carbon nanotube. Charge correlations ($\bar{\chi}_{CDW}^{-,M}$ and $\bar{\chi}_{CDW'}^{-,M}$) are in all cases the most divergent and open a pseudo-gap which subdues the superconducting fluctuations. The introduction of Coulomb interactions, through u and b , reinforces this tendency even more. Kociak *et al.*⁶, however, mention the possibility that the band occupancy might not be exactly 1/2. If this were the case, as far as we can estimate from a tight-binding calculation, the sign constraints mentioned in Eq. (3) still hold. However, the Fermi level would shift by $\Delta E = dv_F k_F/2$ (d is the doping level) and the two bands would have different Fermi momenta. As a consequence, for energy scales below ΔE the $\bar{g}_i^{(3)}$ would vanish because of longitudinal momentum conservation. Moreover, the interband backward scattering $g_{1,ph}^{(2)}$, which was previously zero (see Eq.3), now is $\sim d^2 g_1$. We now use a three cutoff procedure $W > \hbar\omega_{ph} > \Delta E$, which applies up to 8% doping level where $\Delta E \approx \hbar\omega_{ph}$. In the case where only the phonon mediated interactions are considered we have estimated¹⁰ $\bar{g}_1 = -0.3/n$ and $\bar{g}_2 = \bar{g}_4 = -0.1/n$. Superconducting correlations $\bar{\chi}_{SS}^{-,M}$ are found to dominate for ℓ ($= \ln(W/T)$) greater than a critical ℓ_s ($= \ln(W/T_s)$). This is shown for a typical run in Fig. 2 (only those giving the largest enhancement are shown). Fig. 3 shows the crossover temperatures T_s below which this occurs for various doping levels and different diameter SWCNTs. The turning on of the Coulomb

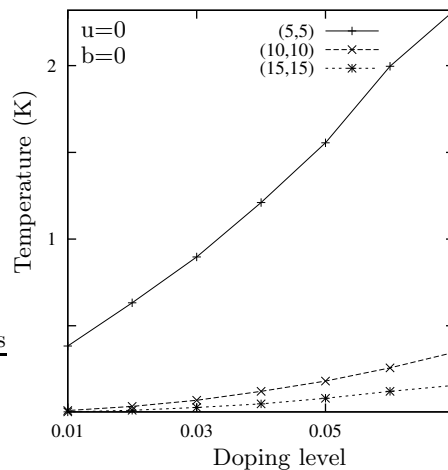


FIG. 3: Temperature at which the superconducting fluctuations dominate as a function of the doping level for three (n,n) armchair tubes. Only phonon-mediated interactions are considered.

interaction lowers T_s and eventually destroys the superconducting fluctuations dominance for $u \gtrsim |g_1|$. At this point, we can conclude that superconducting fluctuations in single armchair nanotubes originating from a phonon mechanism are possible at an appreciable doping level provided the Coulomb interaction is very small. This last condition seems restrictive in view of our own evaluation $u \gg |g_1|$ and the evidence of strong electronic correlations in SWCNT¹⁵. Moreover, the finite length of the nanotubes results in a discretization of the energy levels¹⁶. Consequently, the energy scale in the renormalization group procedure cannot be smaller than this spacing. We estimate this would occur at best at 1K which is still larger than the temperatures at which the work of Kociak⁶ shows any indication of superconductivity. It thus seems likely that the superconductivity seen in ropes takes place by a coupling effect between the nanotubes. At the dimensionality crossover temperature $T_x \sim t_{\perp}/\pi$, where t_{\perp} is the net inter-tube hopping amplitude, inter-tube hopping becomes coherent¹⁷. Any fluctuating superconducting pair that might exist will thereafter be able to coherently tunnel between tubes. This surely occurs much before the SWCNT discrete spectrum is felt. The single tube superconducting fluctuations need not be dominant for this to take place. The existence of frustration in ropes of close packed SWCNT would prevent the further development of bond-order wave deformations (associated with a Kekule CDW modulation¹⁰) or magnetic order and allow superconductivity to develop. Moreover, the interchain particle-hole interactions that might exist at T_x could also play a role in enhancing superconductivity through a mechanism similar to the one proposed for organic materials^{17,18}. All of this is consistent with the small temperatures observed for superconductivity in ropes of armchair nanotubes.

The recent discovery of superconducting fluctuations

at 15 K in a single (5,0) zigzag SWCNT¹⁹ thus seems puzzling in view of the above analysis of armchair nanotubes. In this specific instance, the very strong $\sigma-\pi$ hybridization due to the very small diameter of the SWCNT changes the band structure in a dramatic way and makes the tubes metallic instead of being the expected insulating state². The band structure might share similarities with the one in a conducting (6,0) zigzag SWNT²⁰. The band structure in the vicinity of the Fermi level would then show the crossing between a non-degenerate band (1) and doubly-degenerate bands (2,3) of opposite curvature and having a different transverse angular momentum. Because of the twofold degeneracy, the Fermi level no longer lies at the crossing point but is offset so that the bands (1) and (2,3) have different Fermi momenta. Moreover, the tight symmetry relationship of the armchair bands exists no longer between (1) and (2,3). There are also many different phonons contributing to effective phonon-mediated electron-electron interactions. Finally, all $\bar{g}_i^{(3)}$ will vanish because of longitudinal momentum conservation. This, we believe, is quite sufficient to allow for important superconducting fluctuations in the zigzag tubes. Purely as an illustration and only for crude order of magnitude estimates, we used the model developed above with only two cutoffs $W = \Delta E \sim 0.3\text{eV}$ ²⁰,

$\hbar\omega_{ph} \sim 0.166\text{eV}$, and $n = 3$ to account for the smaller tube diameter such that $\bar{g}_1 = -0.1$, $\bar{g}_2 = -0.03$. We find a dominance of the superconducting response below room temperature with just the phonons. This is much larger than for the armchair tubes and might explain the origin of the superconducting fluctuations observed by Tang *et al.*¹⁹. But again adding a Coulomb interaction quickly reduces this temperature. Superconductivity disappears again for $u \gtrsim |g_1|$. The results of Tang would thus indicate an unexpectedly small Coulomb interaction in zig-zag nanotubes. A more detailed analysis of the three-band RG will be given elsewhere.

Acknowledgments

The authors thank D. Senechal for useful comments and discussions on several aspects of this work. We also thank the National Sciences and Engineering Research Council of Canada (NSERC), le Fonds pour la Formation de chercheurs et l'Aide à la Recherche du gouvernement du Quebec (FCAR) and the "Superconductivity program" of the Institut Canadien de Recherches Avancées (CIAR), for financial support.

¹ S. Ijima, *Nature* **354**, 56 (1991).

² R. Saito, G. Dresselhaus, and M. S. Dresselhaus, *Physical Properties of Carbon Nanotubes* (Imperial College Press, 1998).

³ N. Hamada, S. I. Sawada, and A. Oshiyama, *Phys. Rev. Lett.* **68**, 1579 (1992); K. Tanaka, K. Okahara, M. Okada, and T. Yamabe, *Chem. Phys. Lett.* **191**, 469 (1992); H. Ajiki and T. Ando, *J. Phys. Soc. Jpn.* **62**, 1255 (1993); C. T. White and J. W. Mintmire, *Nature (London)* **394**, 29 (1998); R. Saito, M. Fujita, G. Dresselhaus, and M. S. Dresselhaus, *Phys. Rev. B* **46**, 1804 (1992); C. White, D. H. Robertson, and J. W. Mintmire, *Phys. Rev. B* **47**, 5485 (1993); J. W. Mintmire and C. T. White, *Phys. Rev. Lett.* **81**, 2506 (1998).

⁴ J. W. Mintmire, B. I. Dunlap, and C. T. White, *Phys. Rev. Lett.* **68**, 631 (1992).

⁵ M. Bockrath *et al.*, *Science* **275**, 1922 (1997); T. W. Ebbesen *et al.*, *Nature (London)* **382**, 54 (1996); S. J. Tans *et al.*, *ibid.* **386**, 474 (1997); T. W. Odom, J. Huang, P. Kim, and C. M. Lieber, *ibid.* **391**, 62 (1998); J. W. G. Wildöer *et al.*, *ibid.* **391**, 59 (1998).

⁶ M. Kociak *et al.*, *Phys. Rev. Lett.* **87**, 75501 (2001).

⁷ C. Journet *et al.*, *Nature (London)* **388**, 756 (1997); L. Vaccarini *et al.*, *C. R. Acad. Sci.* **327**, 925 (1999).

⁸ J. Solyom, *Adv. Phys.* **28**, 201 (1979).

⁹ C. Bourbonnais and L. Caron, *International Journal of Modern Physics B* **5**, 1033 (1991).

¹⁰ A. Sedeki, L. G. Caron, and C. Bourbonnais, *Phys. Rev. B* **62**, 6975 (2000).

¹¹ R. A. Jishi, M. S. Dresselhaus, and G. Dresselhaus, *Phys. Rev. B* **48**, 11385 (1993).

¹² Y. A. Krotov, D.-H. Lee, and S. G. Louie, *Phys. Rev. Lett.* **78**, 4245 (1997).

¹³ R. Egger and A. O. Gogolin, *Phys. Rev. Lett.* **79**, 5082 (1997).

¹⁴ L. G. Caron and C. Bourbonnais, *Phys. Rev. B* **29**, 4230 (1984).

¹⁵ S. J. Tans, M. H. Devoret, R. J. A. Groeneveld, and C. Dekker, *Nature (London)* **394**, 761 (1998).

¹⁶ M. Bockrath, D. Cobden, P. McEuen, N. Chopra, A. Zettl, A. Thess, and R. Smalley, *Science* **275**, 1922 (1997).

¹⁷ V. J. Emery, *Synthetic Metals* **13**, 21 (1986); C. Bourbonnais and L. Caron, *Physica B* **143**, 450 (1986).

¹⁸ C. Bourbonnais and L. Caron, *Europhys. Lett.* **5**, 209 (1988).

¹⁹ Z. K. Tang *et al.*, *Science* **292**, 2462 (2001).

²⁰ X. Blase, L. X. Benedict, E. L. Shirley, and S. G. Louie, *Phys. Rev. Lett.* **72**, 1878 (1994).